Biofunctional Silk/Neuron Interfaces

Valentina Benfenati, Katja Stahl, Carolina Gomis-Perez, Stefano Toffanin, Anna Sagnella, Reidun Torp, David L. Kaplan, Giampiero Ruani, Fiorenzo G. Omenetto, Roberto Zamboni, and Michele Muccini**

Silk fibroin (SF) is a biocompatible and slowly biodegradable material with excellent mechanical properties and huge potential for use as biofunctional interface in electronic devices that aim to stimulate and control neural network activity and peripheral nerve repair. It is shown that SF films act as material interfaces that support the adherence and neurite outgrowth of dorsal root ganglion (DRG) neurons and preserve neuronal functions. Silk films preserve the capability of neuronal cells to fire and DRG neurons on silk films retain the intracellular free Ca^{2+} concentration ($[Ca^{2+}]_i$) response to capsaicin, a typical noxious stimulus for this neuronal culture model. It is also demonstrated that nerve growth factor (NGF)-functionalized silk films promote neurite outgrowth and modulate functional properties of DRG neurons. The results show that silk preserves DRG neuronal physiology and is a promising biomaterial platform for the future development of devices with goals including functional recovery of injured neurons, neurite functional outgrowth in vitro, or functional electrostimulation in vivo.

1. Introduction

Neuronal cells are electrogenic cells of the nervous system that have attracted increasing attention as potential interfaces for electronic devices targeted at neuroscience investigation and applications.[1,2] A wide range of pathophysiologies can be treated by stimulation of the nervous system, including hearing loss, chronic pain, and peripheral nerve injury (PNI).[3] However, solutions to many critical problems in neural biology/medicine are limited by the availability of specialized materials with suitable mechanical, chemical, and biocompatibility properties that are critical for integration with neural tissue in, e.g., long term implants.[4,5]

Electrical stimulation is another therapeutic treatment for PNI to stimulate neurite and axon extension or nerve regeneration in vitro and/or in vivo.[3,6] In this rapidly emerging area, particular attention is devoted to the engineering and use of interfaces that can be integrated in biocompatible electronic devices.[7] However, achieving a thorough biocompatibility can be challenging due to the complex nature of the biological response to interaction with many organic and inorganic materials. A clear understanding of the interaction of neural cells at the interface with their environmental support will allow engineering of tissues, which effectively can mimic in vivo cell–matrix and cell–device interactions. An interface suitable for nerve regeneration should support neurite outgrowth and preserve and promote functional recovery of neuronal cells (biofunctional interface), in particular by enabling neuronal conduction of action potential. To this end, in vivo electrophysiological protocols, such as analyses of compound muscle action potential (CMAP), are currently performed on rat animal models.[8–11] However, histomorphometric or CMAP in vivo measurements correlate poorly with the functional recovery of patients.[10]

Alternatively, the bioelectrical activity of peripheral neurons can be monitored in vitro to study functional neuroregenerative mechanisms promoted by biomaterials employed in neural-integrated devices. Control of bioelectrical properties underpinning neuronal firing of injured peripheral neurons is crucial to define a primary pharmacological target in neuroregenerative medicine in order to rescue the function of neural networks.[12,13] Moreover, it is now evident that both inhibition of specific bioelectrical properties and intracellular calcium ($[Ca^{2+}]_i$) dynamics of afferent primary sensory neurons are realistic targets to inhibit chronic pain that develops after traumatic PNI.[14,15]

Therefore, by combining biomaterial grafts with proper active molecules, a passive scaffold might turn into an active platform that supports neurite outgrowth and delivers substances

Dr. V. Benfenati, Dr. S. Toffanin, Dr. G. Ruani, Dr. M. Muccini
Consiglio Nazionale delle Ricerche (CNR)
Istituto per lo Studio dei Materiali Nanostrutturati (ISMN)
via Gobetti, 101, 40129, Bologna, Italy
E-mail: v.benfenati@bo.ismn.cnr.it; M.Muccini@bo.ismn.cnr.it
K. Stahl, Prof. R. Torp
Center for Molecular Biology and Neuroscience
University of Oslo
P.O. Box 1105 Blindern NO-0317 Oslo, Norway
Dr. C. Gomis-Perez
Department of Human and General Physiology
University of Bologna
via S. Donato 19/2, 40127, Bologna, Italy
A. Sagnella, Dr. R. Zamboni
Consiglio Nazionale delle Ricerche (CNR)
Istituto per la Sintesi Organica e la Fotoreattività (ISOF)
via Gobetti, 101, 40129, Bologna, Italy
Prof. D. L. Kaplan, Prof. F. G. Omenetto
Department for Biomedical Engineering
Tufts University
Medford, MA 02155, USA

DOI: 10.1002/adfm.201102310

© 2012 WILEY-VCH Verlag GmbH & Co. KGaA, Weinheim

targeted to promote the proper recovery or modulates functionality of injured neurons, ultimately alleviating painful disabilities. To reach this goal the biomaterial scaffold/delivery system must preserve bioelectrical properties of neuronal cells, enabling action potential generation and retaining chemosensitivity to specific environmental stimuli.

Despite the plethora of data regarding cell viability and neurite outgrowth in vitro, there is a lack of knowledge concerning the effects that interacting materials may exert on neuronal function per se.

Silk fibroin (SF) has several remarkable and well-documented characteristics, including mechanical flexibility, biocompatibility, controllable biodegradability, dielectric properties, and the capability for drug stabilization and release.[16–18]

SF-based biomaterials have recently found increasing applications in tissue engineering, including the generation of artificial nerve guides for peripheral nerve repair.[9,20,21] Silk fibroin matrices provide controlled release of nerve growth factor (NGF). By combining silk films with NGF, the adherence and metabolic activity and neurite outgrowth of the neuronal cell line PC12 was supported.[19] Moreover, the feasibility of using purified silk fibroin fibers to construct artificial nerve grafts has been evaluated by testing the biocompatibility of SF material with peripheral nerve tissues and cells.[20,21] Dorsal root ganglia have been cultured on SF fibers and cell outgrowth from DRGs was demonstrated by using light and electron microscopy coupled with immunocytochemistry and biochemical assay analyses.[21] Of note, DRG sensory neurons and spinal cord motor neurons from chicken embryos exhibited an extended length and rate of axonal outgrowth parallel to the aligned silk nanofibers loaded with glial cell line-derived neurotrophic factor (GDNF) and NGF.[20] Moreover, ultrathin films of SF have been demonstrated to function as integrated components in advanced implantable biomedical devices in vivo.[22,23] Finally, we recently showed that silk films do not induce reactive astrogliosis in vitro, a reaction that could seriously compromise prosthetics device performance.[24]

All of this evidence indicates that silk fibroin is a highly promising biomaterial to be employed as an in vivo graft/device platform in PNI repair therapy. However, there is a lack of knowledge concerning the effect that silk exerts on the bioelectrical properties of peripheral neurons, which is essential to define silk as a novel technological platform in PNI repair. Here, we report on the effects exerted by silk on peripheral neuron electrophysiological properties and, in particular, on the action potential of primary sensory neurons, the bodies of which are located in DRG. We used whole-cell patch-clamp techniques to assess the electrophysiological characteristics of rat DRG neurons plated on silk-films, with the well known reference system poly-D-lysine (PDL) plus laminin seeded cells as the baseline.[25–27] Moreover, we verified that DRG neurons on silk films preserve $[Ca^{2+}]_i$ response to capsaicin, a typical noxious stimulus and a target for pharmacological strategies against neuropathic pain related to PNI.[25,28] After defining the functional properties of neurons in silk films, we induced modification of these cells by plating DRG neurons on silk films embedded with nerve growth factor (NGF). Our results demonstrate the capability of SF+NGF substrates to stimulate neurite outgrowth and to modulate bioelectrical properties as well as chemoresponsiveness of DRG neurons, thus showing that silk serves as a biofunctional material interface for devices intended for the nervous system in vivo or to generate models to study PNI in vitro.

2. Results and Discussion

2.1. Silk Fibroin Film Characteristics

The first step of our study was to characterize the structure of silk fibroin films since it is known that SF molecular conformation influences the degradation of the protein contained in silk.[29,30] To this end, the structure of silk films was determined using Fourier transform infrared (FTIR) spectroscopy. The infrared spectral region from 1700–1200 cm^{-1} (**Figure 1**a) was previously assigned to absorption of the peptide backbones of amide I (1700–1600 cm^{-1}), amide II (1600–1500 cm^{-1}), and amide III (1350–1200 cm^{-1}) and used for the analysis of different secondary structures of silk fibroin.

The amide I band appeared as a strong peak at 1660 cm^{-1}, corresponding to silk I structure. In the amide II region, peaks were seen at 1531 cm^{-1} (silk I) and at 1515 cm^{-1} (silk II). In the amide III region, a peak at 1235 cm^{-1}, generally assigned to random coil-structures, is observed.[29,30] These data indicate that the conformational structure of the protein in SF films resembles those previously reported for films prepared using slow drying methods in which there is a dominance of the silk I structure (random coils and alpha helices) with respect to the silk II.[29]

As the in vitro cell culture environment could potentially affect the characteristics of the biomaterial interfacing cultured cells, we next sought to analyse the effect of cell culture treatment on silk films after exposure to in vitro cell culture treatment, i.e., maintenance in cell culture media, and in a biological incubator (37 °C, 5% CO_2). The morphology of SF at different time points after exposure to this treatment was analyzed using atomic force microscopy (AFM) in air after drying the sample at 60 °C for 1 h.

AFM analysis showed that untreated silk films (Figure 1b) have light-grainy morphology, comparable to that of previously reported cast silk films.[31] After 3 days of treatment (Figure 1c), nanoparticles and short nanofilaments of SF were visible in the substrate, but they were rarely visible after 7 days (Figure 1d). The relative root mean square (rms) roughness value of the silk layer increases from 0.7 nm (Figure 1b, not treated) and to 10 nm after 3 days (Figure 1c), then decreases to 2 nm after 7 days (Figure 1d). We also evaluated the degradation of silk films by quantitative weight loss measurements of silk films at different time points (Figure 1e). After 24 h, the weight loss of the silk films was ≈50% (53 ± 0.8%), then it reached a plateau value of ≈60% (61.7 ± 6) after 3 days, remaining constant until day ten.

These data suggest that conformational, morphological and dissolution rate properties of SF films are compatible with in vitro cell culture standard conditions for maintenance and analysis of primary sensory neurons.[32]

© 2012 WILEY-VCH Verlag GmbH & Co. KGaA, Weinheim

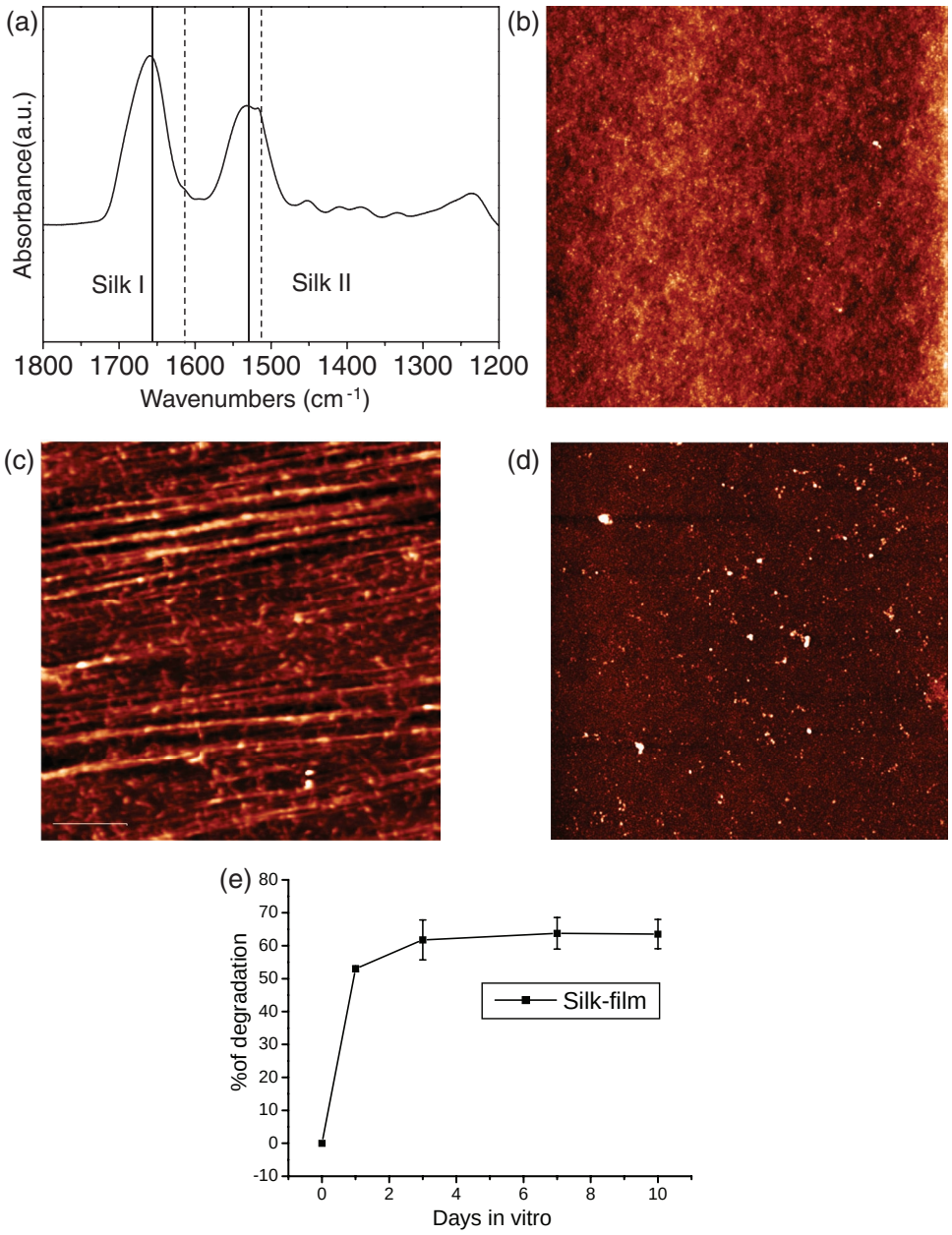

Figure 1. a) FTIR spectra of silk films. Continuous lines refer to silk I peaks, dashed line to silk II conformational structure of silk protein. b–d) AFM images of silk films before (b), 3 days after (c), and 7 days after (d) in vitro cell culture treatment. Scale bar: 2 µm. e) Dissolution of SF films over time. Data are reported as mean ± standard error (S.E.) of percentage of weight loss measured in three samples for each time point.

2.2. Silk Films Enable DRG Neuron Growth and Differentiation

DRG contains a heterogeneous population of primary sensory neurons that convey information about a variety of sensory stimuli, including touch, temperature, and pain.[12,13,33] Cultures of dissociated rat DRG neurons are a validated model to determine the regenerative outgrowth capabilities of individual neurons of the peripheral nervous system (PNS) in the presence or absence of in vivo pre-nerve injured lesions.[12,13] Moreover, many of the functional properties of nociceptive neurons in vivo, involved in PNI related pain disease, are known to be replicated in small cultured neurons from the DRG.[33]

Thus, we sought to culture DRG primary neurons from postnatal rats on silk-film-coated glass coverslips. As control, half of the DRG preparations were cultured on PDL+laminin-treated glass coverslips.[26,27] Cell culture preparations imaged after 3, 5, and 9 days in vitro (div) are reported in **Figure 2**. Immediately after plating, neuronal cell bodies typically appeared rounded, with a small proportion of neurons retaining short axonal stumps under both experimental conditions (data not shown),

© 2012 WILEY-VCH Verlag GmbH & Co. KGaA, Weinheim

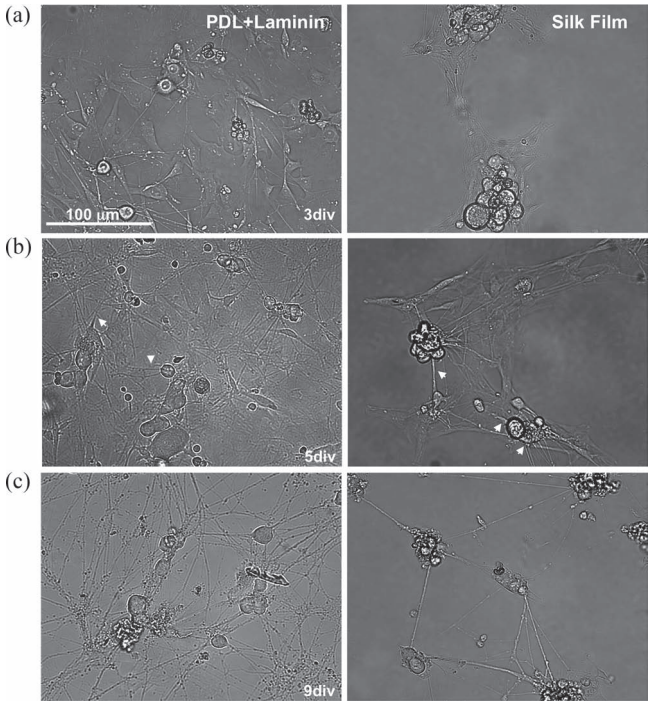

Figure 2. a–c) Microscopy images representing morphological observations performed on PDL+laminin-plated (left panel) and silk-plated DRG cultures (right panels) at different time points. a) After 3 days in vitro (div). b) After 5 div. Arrowheads indicate neurite outgrowth c) After 9 div, showing the formation of dense network connections. Scale bar is 100 µm.

resembling the typical behavior of DRG cell cultures.[34,35] Morphological observations of PDL+laminin cultured cells after 3 div showed spread neurons with different diameters for the cell bodies (Figure 2a, left panel) and process extensions on a layer of glial cells. Marked neurite outgrowth was observed after 5 div (Figure 2b, left panel) evolving into a dense network of connections after 9 div (Figure 2c,d, left panels).

After 3 div the SF cultured cells displayed more pronounced rounded shape clusters of DRG neurons with very short stumps (Figure 2a, right panel) compared to the PDL+laminin cultured cells. Of note, axonal outgrowth appeared clearly from clustered cells after 5 days (Figure 2b, right panel), which further developed into elongations to form a dense network after several days in culture (Figure 2c, right panel).

During the culturing process, cell viability and cell number was measured (**Figure 3**). Single plane confocal images of fluorescein diacetate assay (FDA) stained cells revealed that viable cells were clearly visible in both DRG preparations (Figure 3a,b). Higher magnifications revealed that cells showing a typical DRG morphological phenotype[35] grew on SF (Figure 3d). Furthermore, neuronal cells grown on silk films were more clustered than those grown on control substrate (Figure 3c). Notably, the total number of cells after 3 div as well as 7 div was not significantly different under the two experimental conditions (Figure 3e: cell number per unit area was 26 ± 4 and 18 ± 4 for PDL+laminin and SF, respectively, after 3 days; 10 ± 1 for PDL+laminin, and 11 ± 2 for SF cells after 7 days).

To verify the presence of neuronal cells in primary DRG cultures, immunofluorescent staining was performed using an antibody against neuronal nuclear protein (NeuN), a typical marker expressed by mature neurons.[36,37] Single plane confocal imaging of NeuN positive cells from PDL+laminin (Figure 3f) and silk film DRG cultures (Figure 3g) are shown in Figure 3. Most of the rounded cells showing a DRG morphological phenotype[35] were NeuN positive. Of note, the overall number of NeuN positive cells was not significantly different between PDL+laminin and silk films plated cells (Figure 3h).

Growth-associated protein GAP43 is a major constituent of the axonal growth cone and is expressed in cell bodies and outgrowing neurites of fetal and neonatal rat brain and DRG sensory neurons.[38] This protein is used as marker for axonal growth. Typical single plane confocal images of immunostained GAP43 from PDL+laminin and silk cultured cells after 5 div are shown in **Figure 4**. GAP43 was highly expressed in the cell bodies and neurites (Figure 4a,b, white arrows) of both cell culture types, demonstrating the occurrence of axonal outgrowing and regenerating processes in the cells cultured on silk films. We also quantified and compared neurite length after 3 div and 5 div (Figure 4c) in both experimental conditions. The average neurite length was significantly lower in silk fibroin plated neurons after 3 days, whereas the length was comparable after 5 days. These data are compatible with a consistent outgrowth of process extensions of DRG neurons grown on silk films, clearly indicating that silk films promote a scaffold for neurite outgrowth.

Peripheral nerve repair after traumatic or degenerative nerve injury remains a challenging clinical problem and recovery strictly depends on the degree of lesion.[39–41] In the case of large nerve gaps, where end-to-end suturing is not indicated, the current gold standard treatment involves the implantation of nerve autografts to bridge the proximal and distal nerve stumps.[39] This approach facilitates nerve regeneration and promotes the rescue of nerve function.[40] Nerve conduits embedded with axonal outgrowth promoting agent, such as neurotrophins, have been developed.[42] The feasibility of using purified SF fibers to construct artificial nerve grafts has been evaluated by testing the biocompatibility of SF material with peripheral nerve tissues and cells.[20,21] The bioengineering of biological or synthetic scaffolds for nerve reconstruction by enrichment with glial/Schwann cells has also been investigated.[43] In this context, previous studies have defined the biocompatibility of silk for DRG cells.[20,21] The present study demonstrates that NeuN positive cells from DRG cell culture preparations grow on bare silk fibroin films.

Despite a more clustered distribution of neurons after 3 div, the morphological behavior of DRG neurons was comparable after several days in vitro under the two experimental conditions (Figure 2). The neurite outgrowth appeared later (3–5 div) in the SF cultures. Our data on neurite length (Figure 4) agree with previous comparative analyses of DRG neuronal differentiation on different protein substrates.[32] Noteworthy is the demonstration that silk films are permissive neuron interfaces that enable DRG neuron adhesion and differentiation in vitro.

These data pave the way for the use of silk as a platform material for devices intended for selective studies of neuronal

© 2012 WILEY-VCH Verlag GmbH & Co. KGaA, Weinheim

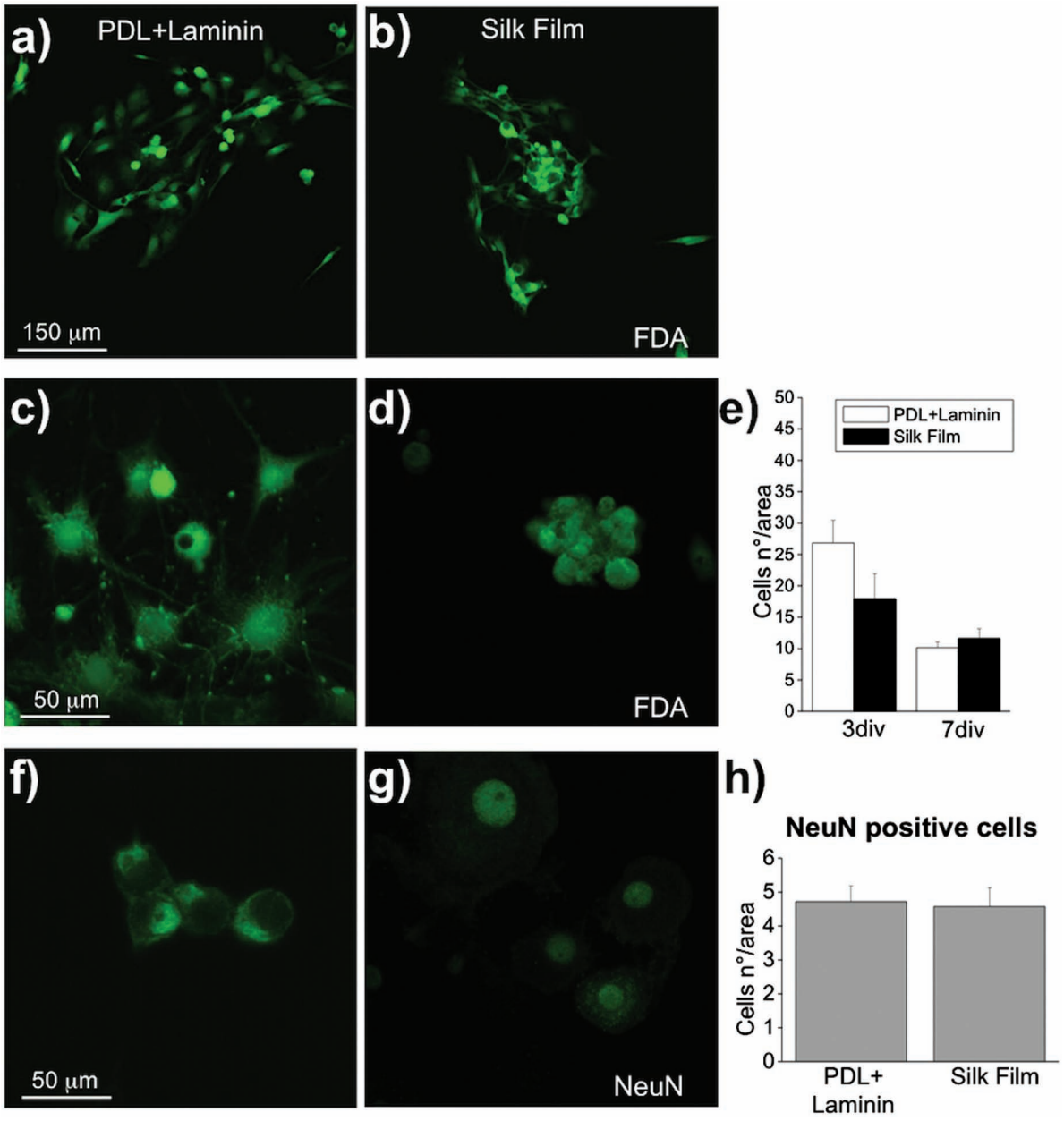

Figure 3. a,b) Single plane 20× confocal images of FDA-stained DRG cells plated on PDL+Laminin (a) and on silk film (b), captured after 3 days in vitro. c,d) High magnification images (60×) of the two cell culture preparations showing the typical DRG neuron morphology. e) Histogram plot of the number of FDA positive cells/areas counted in PDL+laminin (black bars) and silk film (white bars) cell culture preparations. f,g) Single plane confocal images of PDL+laminin (f) and silk-films (g)-plated DRG cells, stained for the neuronal marker NeuN. h) Histogram plot of the number of NeuN positive cells/area.

cell regeneration or analyses of neuronal cell function. In agreement with previous studies,[35] we observed that the number of non-neuronal cells was highly variable from sample to sample under both experimental conditions.

Since our focus was to test the effect of silk on primary sensory neurons function, we added Ara-C to the cell culture media to suppress the expression of proliferating (glial) cells, that exert a well-known trophic effect on neuronal growth.[27,44] Our experimental paradigm is thus not aimed at investigating silk as a platform for the growth of peripheral glial cells. However, we did not observe differences in the overall number of NeuN positive cells in the different preparations between PDL+laminin and silk plated cells (Figure 3). In agreement with previous findings on hippocampal neurons from the central nervous system (CNS),[45] we observed a high level of expression of GAP43, a protein marker of axonal neurite outgrowth,[38] as an indication of neural differentiation in DRG neurons cultured on the silk films.

© 2012 WILEY-VCH Verlag GmbH & Co. KGaA, Weinheim

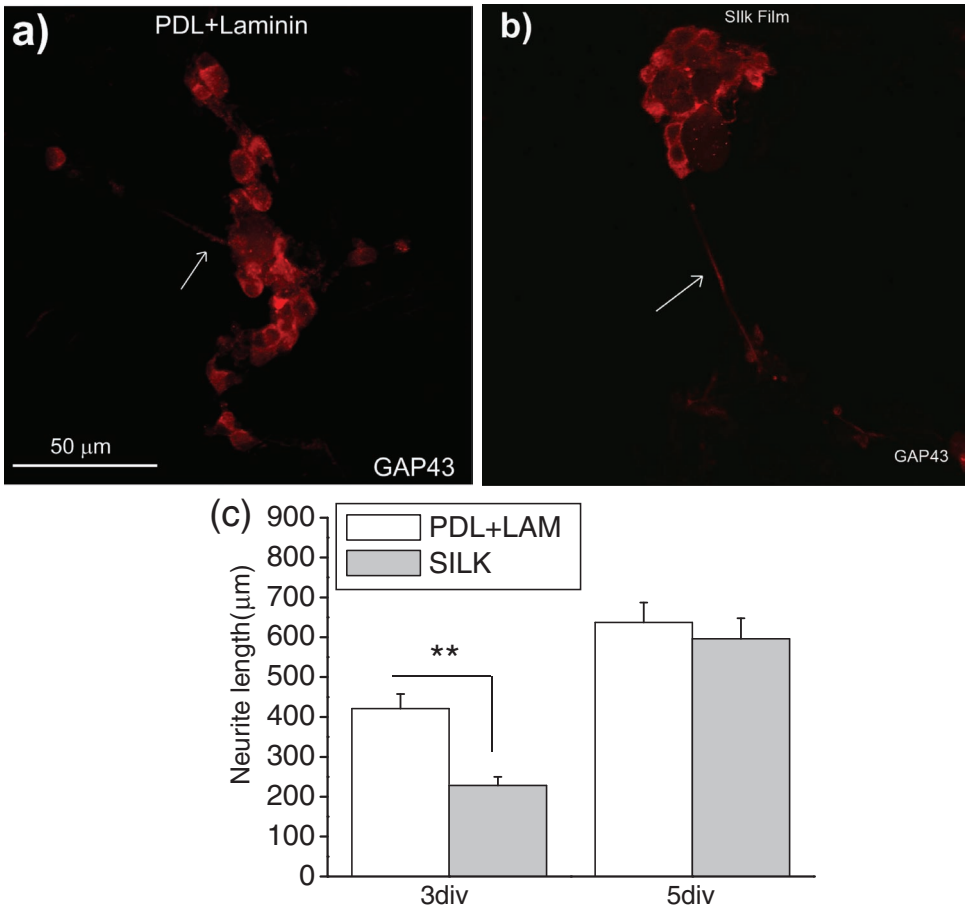

Figure 4. a,b) Typical single plane confocal images of immunostaining for the axonal outgrowth marker GAP43 on PDL+laminin (a) and silk cultured neurons (b) after 5 days in vitro (div). Scale bar is 50 μm. c) Histogram plot showing neurite length measured after 3 div and 7 div in PDL+laminin (white bars) and silk film cultured neurons (gray bars). Significant difference was observed in mean values after 3 div; $n = 42$ and 40 for 3 div measurement and $n = 38$ and 40 for 7 days (n is the number of cells analyzed).

2.3. Electrophysiological Properties of DRG Neurons on Silk Films

In order to analyze the effect of silk on DRG neuron electrophysiological properties, whole-cell patch-clamp experiments were carried out on DRG neurons after 3 days on PDL+laminin and silk-film-plated cells. With control intracellular and extracellular saline, cells were held at –60 mV and increasing current pulses of 50 pA were injected from 50 to 350 pA amplitude for a duration of 100 ms (**Figure 5**a) or 1 s (Figure 5b). Figure 3 shows current-clamp traces relative to voltage amplitude behavior of the first action potential evoked from PDL+laminin cultured neuron (left panels) in response to a pulse family of 100 ms duration. Of note, the same protocol applied in silk-film-plated cells (right panels) enables neuronal depolarization and induction of action potentials. In agreement with previous studies,[46,47] the firing pattern of patched neurons was variable under both experimental conditions. At threshold current values, upon long lasting pulse stimulation (1 s) single spiking (phasic firing) (Figure 5b) as well as repetitive firing (Figure 5c) neurons were observed in PDL+laminin (right panels) and silk-film-plated cells (left panels).

A comparative analysis of the average of bioelectrical properties of different PDL+laminin and silk film neurons that were patched is reported in **Table 1**. The passive membrane properties analyzed were the cell capacitance and the resting membrane potential (V_{mem}). Mean values of cell capacitance were recorded in both experimental settings and were in agreement with previously reported data for small diameter DRG neurons (≤30 μm).[48] It is noteworthy that these values were slightly higher in the silk-plated DRG neurons, suggesting a larger cell surface area on silk. A plausible explanation of increased cell capacitance of DRG plated on silk films as compared to PDL+ laminin is the neurite outgrowth of neurons in silk films occurring after 3 days (Figure 3). Indeed it is well known that increased cell capacitance occurs at the beginning of neuronal neurite growth processes where short stumps departing from the cell body could increase the total cell body surface area.[49,50] In this regard, our data agree with morphological and neurite length analyses, which revealed that after 3 div SF DRG neuron outgrowth was in the early phase.

In contrast, the resting membrane potential (V_{mem}) was comparable under the two experimental conditions. The excitability

© 2012 WILEY-VCH Verlag GmbH & Co. KGaA, Weinheim

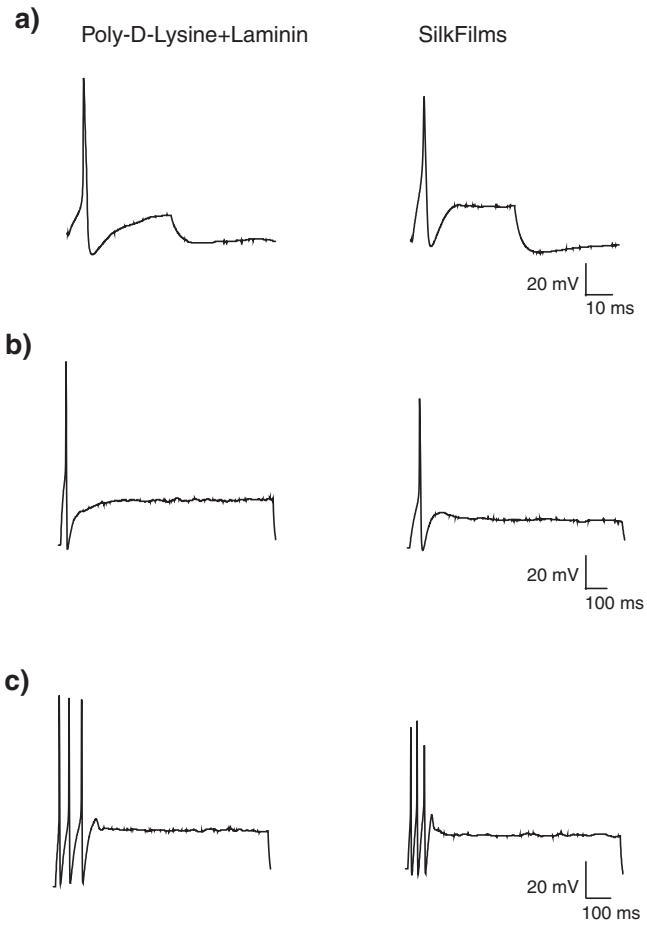

Figure 5. a) Traces representative of voltage amplitude behavior recorded in current-clamp mode of patch-clamp. The first action potential evoked from a PDL+laminin cultured neuron (left panel) and silk film-plated cells (right panels) obtained in response to, a pulse family of 100 ms duration. b,c) Current clamp traces obtained by long lasting pulse stimulation (1 s). Firing pattern of patched neuron was phasic firing (b) as well as repetitive firing (c) neurons in PDL+laminin (left panels) and silk film-plated cells (right panels).

measurements that we analyzed include the AP threshold current (I_{th}) and the AP voltage threshold (V_{th}). These two parameters were not significantly different under the two experimental conditions. We also analyzed the AP peak, AP amplitude, time to peak, number of firing and after hyperpolarization period (AHP) amplitude. Of these, only AP peak and AP amplitude were significantly lower in DRG neurons plated on the silk films.

We also performed voltage-clamp recording current on firing neurons to monitor whole-cell current profiles. The cells were stimulated with 50 ms voltage steps (V_h = –60 mV) from –50 to 60 mV in 10 mV increments (**Figure 6**a, inset). Representative current traces obtained on PDL+laminin and silk-plated DRG neurons in response to the applied voltage are displayed in Figure 6a,b).

Under both experimental conditions voltage-dependent whole-cell currents were composed of fast activating and inactivating inward currents, which were fully activated between –20 mV and –10 mV, followed by slow-activating outward currents that were activated at potentials more positive than –30 mV. Most neurons displayed non-inactivating outward currents, but a transient component was sometimes also observed.

A comparative analyses obtained from a current–voltage (I–V) plot of mean values of peak-current density, recorded for each voltage step (Figure 6c,d), revealed a similar voltage-dependent profile of whole-cell current of PDL+laminin and silk-plated neurons. In both cases the average of threshold voltage for inward current activation was ≈30 mV with a maximal conductance at approximately –10 mV. Significantly, PDL+laminin cultured DRG neuron displayed a twofold higher inward current density at different voltages as well as higher maximum inward conductance ($G_{in\ max}$ = 31.1 ± 8.9 ns pF^{-1} for PDL+laminin, n = 5 and $G_{in\ max}$ = 14.3 ± 3.5 ns pF^{-1} for silk cells, n = 5). In contrast, the average of outward current densities recorded at any voltages applied was not significantly different under the two experimental conditions.

All together the electrophysiological data collected indicated that the silk preserves the function of DRG neurons, with values that agree with previous reports for this type of cell culture.[46–48,51–53] The mean values of resting V_{mem}, I_{th}, V_{th}, and firing number per second were not different between the two culturing protocols, which indicates that neither PDL+laminin treatment nor silk films induce hypoexcitability or hyperexcitability on DRG-cultured neurons.[53] The difference in overall amplitude of the action potential is related to a lower peak amplitude in silk DRG neurons, since no difference was observed in the V_{th}. It should be noted that, despite the difference, the observed values are comparable with those previously reported for other adhesion molecules, such as poly-L-lysine or laminin.[46,51,52] The lower AP peak amplitude in the silk-plated cells could be related to the alteration in whole cell conductance properties.[46] The maximum magnitude of whole-cell inward current density was smaller in the silk-plated cells compared to

Table 1. Passive and excitability properties of neurons plated on PDL+laminin and silk films.

	C_p [pF]	Resting V_{mem} [mV]	I_{th} [nA]	V_{th} [mV]	Peak amplitude [mV]	Time to peak [ms]	AP amplitude [mV]	AHP amplitude [mV]	Max AP number per s
PDL+laminin	18.5 ± 1	–63 ± 9	134 ± 27	–33 ± 3	44 ± 4	4.3 ± 0,7	78 ± 4	20 ± 2	2.1 ± 0.5
Silk Films	25.5 ± 1.8 *	–66 ± 9	178 ± 11	–36 ± 2	29 ± 4 **	5 ± 0.6	66 ± 4 **	24 ± 2	1.5 ± 0.19

Data correspond to mean value and S.E. C_p: Membrane capacitance; Resting V_{mem}: resting membrane potential; I_{th}: threshold current; V_{th}: voltage threshold; AP: action potential; AHP: after hyperpolarization period amplitude. n values were n = 13 for PDL+laminin and n = 13 for silk film. Significant difference was observed in C_p values (* = $p < 0.05$) and in AP peak (** = $p < 0.01$) and AP amplitude values (** = $p < 0.01$).

© 2012 WILEY-VCH Verlag GmbH & Co. KGaA, Weinheim

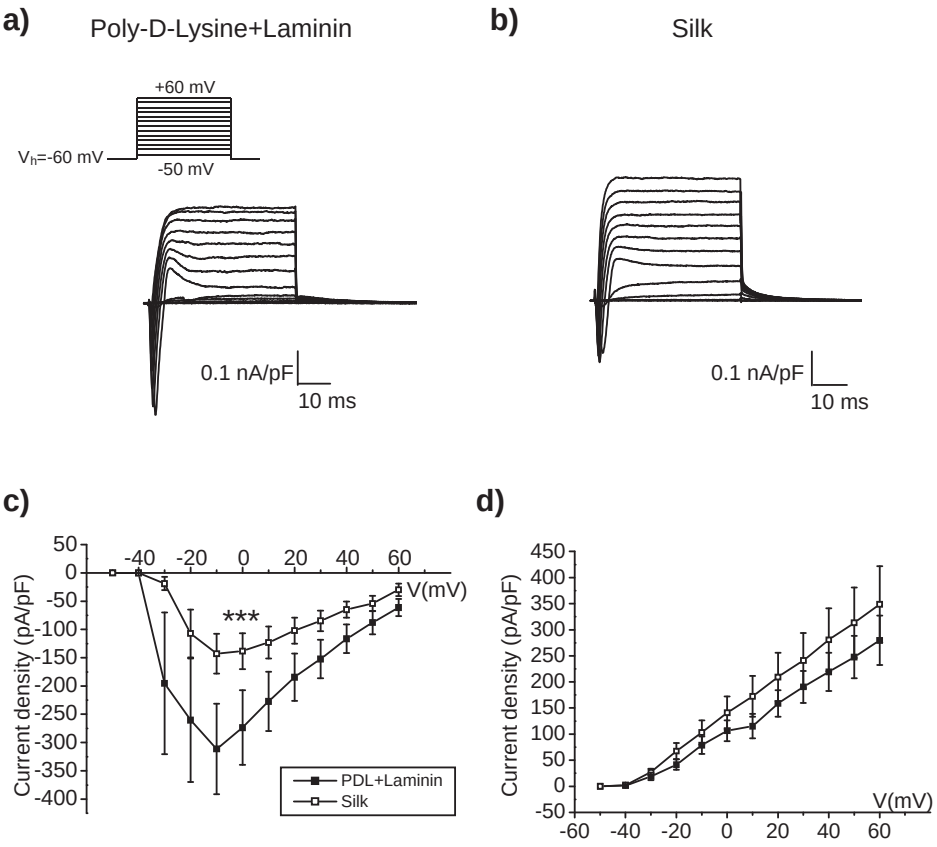

Figure 6. a,b) Current traces recorded stimulating DRG neurons with a family of voltage steps from V_h of –60 mV, from –50 to 60 mV in 10 mV increments (inset). Typical currents depicting whole-cell conductance evoked in poly-D-lysine+laminin neurons (a) and silk-plated neurons (b). Whole-cell currents were composed of fast-activating and inactivating inward currents, by slow-activating and mostly not inactivating outward current. Inward currents were fully activated between –20 and –10 mV and have voltage-dependence comparable in both experimental conditions. The outward potassium current, activated at potentials positive to –40 mV. c,d) Current–voltage (*I–V*) plot: mean values of current intensity (normalized to cell capacitance) recorded at peak in PDL+laminin (black squares) and silk plated-neurons (white squares). c) Inward currents were significantly smaller in silk-plated neurons ($p < 0.001$) in response to potentials between amplitude –20 and 40 mV. d) Outward currents have voltage-dependence and amplitude comparable in both experimental conditions. *I–V* plots have been generated by calculating the average of the maximal inward or outward current values recorded at each potential, and normalized for the relative cell capacitance values ($n = 5$ for PDL+laminin and $n = 5$ for silk).

PDL+laminin plated neurons. However, the voltage-dependent profile of inward conductance was comparable and the time to peak was not significantly different, suggesting that time-dependence properties of ion channels contributing to the depolarizing phase were not altered in silk-DRG neurons. Further studies and detailed analyses of heterogeneous types of sodium channels, contributing to inward conductance expressed in small DRG neurons[54] would clarify whether this is a consequence of either an alteration in expression pattern of ion channels or an increase in their unitary conductance.

2.4. Capsaicin Response of DRG Neurons on Silk Films

DRG-derived sensory neuron culture is a useful model to evaluate the pathogenic mechanisms of peripheral neuropathies and to examine and validate potential therapeutic compounds.[13] An important molecular sensor for pain sensation, expressed in DRG neurons, is the receptor named vanilloid receptor 1, (VR1).[28,33] The latter is a polymodal sensor that specifically responds to capsaicin, the active ingredient of chilli peppers. Capsaicin activation of TRPV1 is known to excite nociceptive neurons, resulting in a burning pain sensation.[28] There is strong evidence for the involvement of TRPV1 in neuropatic pain observed after PNI.[55] Since the functional relevance of TRPV1 activation is associated with its ability to elicit an intracellular calcium($[Ca^{2+}]_i$) increase, we verified whether capsaicin activation of TRPV1 increases $[Ca^{2+}]_i$ in silk DRG neurons. For this purpose we performed a microfluorometric analysis by measuring changes in fluorescence emission ratio of fura 2-loaded silk plated DRG cells (**Figure 7**).

Microfluorimetric analyses of calcium dynamics revealed that exposure to capsaicin (3 μM) promoted $[Ca^{2+}]_i$ responses that vary in temporal dynamics (Figure 7a,b). Typically, we observed a rapid rise in $[Ca^{2+}]_i$, followed by a sustained $[Ca^{2+}]_i$ plateau. However, oscillatory dynamics, as well as decreased time response were also seen, which agrees with previous reports for capsaicin-evoked TRPV1 responses.[56] Histogram

© 2012 WILEY-VCH Verlag GmbH & Co. KGaA, Weinheim

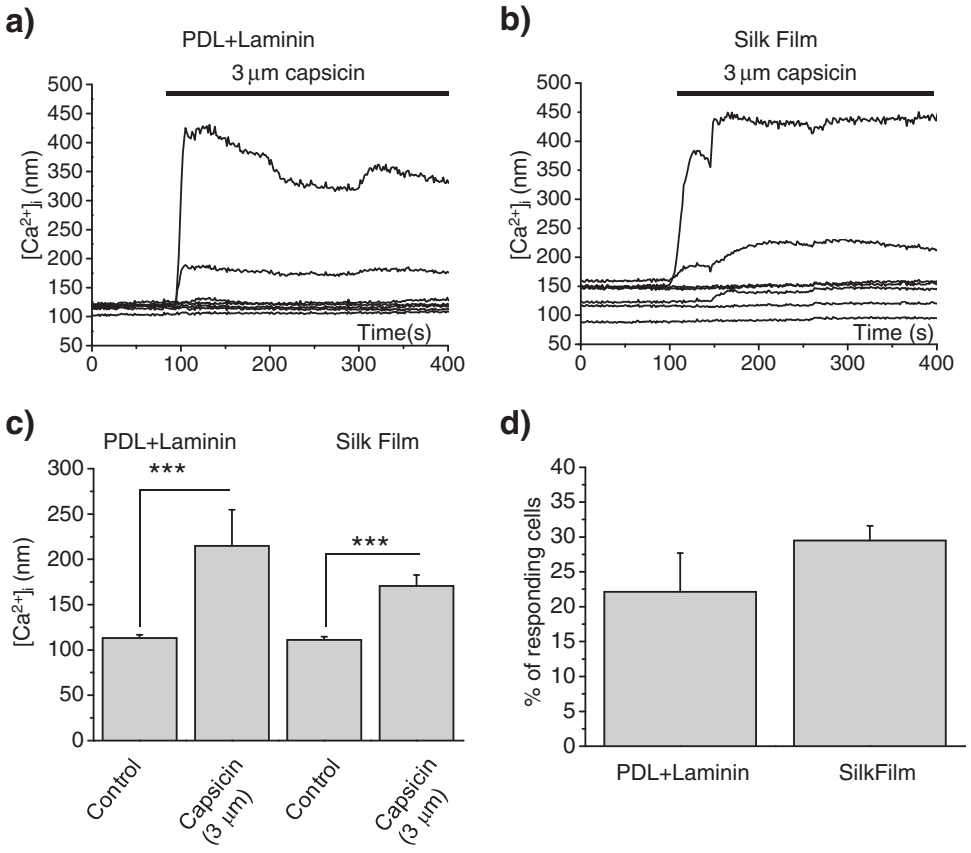

Figure 7. a,b) Representative traces depicting typical temporal dynamics of free intracellular Ca^{2+} concentration ($[Ca^{2+}]_i$) measured in fura-2-loaded DRG cells plated on PDL+laminin (a) or on silk films (b). Each trace corresponds to one cell analyzed in the reported representative experiment. c) Histogram of the mean and SE of $[Ca^{2+}]_i$ values recorded upon control saline and upon addition of 3 μM capsaicin ($n = 23$ for PDL+laminin and $n = 47$ for silk films). d) Percentage of responding cells to capsaicin in PDL+laminin and silk films.

plots of the mean values of ratiometric fluorescence intensity recorded before and after capsaicin, in responsive cells, revealed that capsaicin promoted a significant increase in $[Ca^{2+}]_I$ on PDL+laminin as well as in DRG silk-plated neurons (Figure 7c,d). The response was comparable to those previously reported for DRG neurons plated on different substrates.[33,56] In agreement with previous studies[56] not all the cells responded to capsaicin. It should be noted that TRPV1 and capsaicin-mediated response in DRG cells are functionally restricted to neuronal cells.[57] However, not all DRG neurons, but only those with small diameters are known to respond to capsaicin.[56,58] The percentage of non-responding cells was comparable under the two experimental conditions.

These data indicate that silk preserves chemosensitivity of DRG neurons to TRPV1-mediated noxius stimulus. Therefore, we demonstrated that silk is a biomaterial that does not affect neuronal cell function. Sensation, transduction and firing capability is retained by neurons plated on silk films. Moreover, this is the first demonstration of the functional properties relevant for modulation of cell-interface interaction.

A clear advantage of using SF films is their ability to release embedded molecules and factors that potentially can modulate neuronal cell growth and function.[19,24] In particular, SF matrices provide controlled release of nerve growth factor (NGF). It has been shown that silk films combined with NGF provide support and induce adherence, metabolic activity, and neurite outgrowth of the neuronal cell line PC12.[19]

In this context, we next sought to prepare SF films containing NGF (50 ng mL^{-1}) and compare the effects on DRG neurons to cells grown on bare silk films, where NGF was just added in the cell culture media (**Figure 8** and **Figure 9**). A cell viability assay demonstrates an increased number of viable cells among FDA-stained cells plated silk+NGF films, as compared to bare silk films (Figure 8a,b). The total number of cells was significantly higher after 3 days and 7 days (Figure 8c: cell n° per area = 18 ± 4 for SF and 46 ± 5 for SF+NGF after 3 days; 10 ± 1 and 23 ± 6 for SF and SF+NGF after 7 days).

Additionally, we measured and compared neurite length after 3 div and 5 div (Figure 8d). Of note, the neurite length was almost doubled in DRG plated on silk films+NGF at both time points. Our results clearly show that silk+NGF promote faster neurite outgrowth of DRG neurons, in addition to longer neurite length. Our data are agree with previous studies of neural cell lines and non-mammalian cell cultures, which demonstrated that silk films are composed of a matrix capable of releasing trophic factors and promoting neural cell differentiation and regeneration.[19–21]

© 2012 WILEY-VCH Verlag GmbH & Co. KGaA, Weinheim

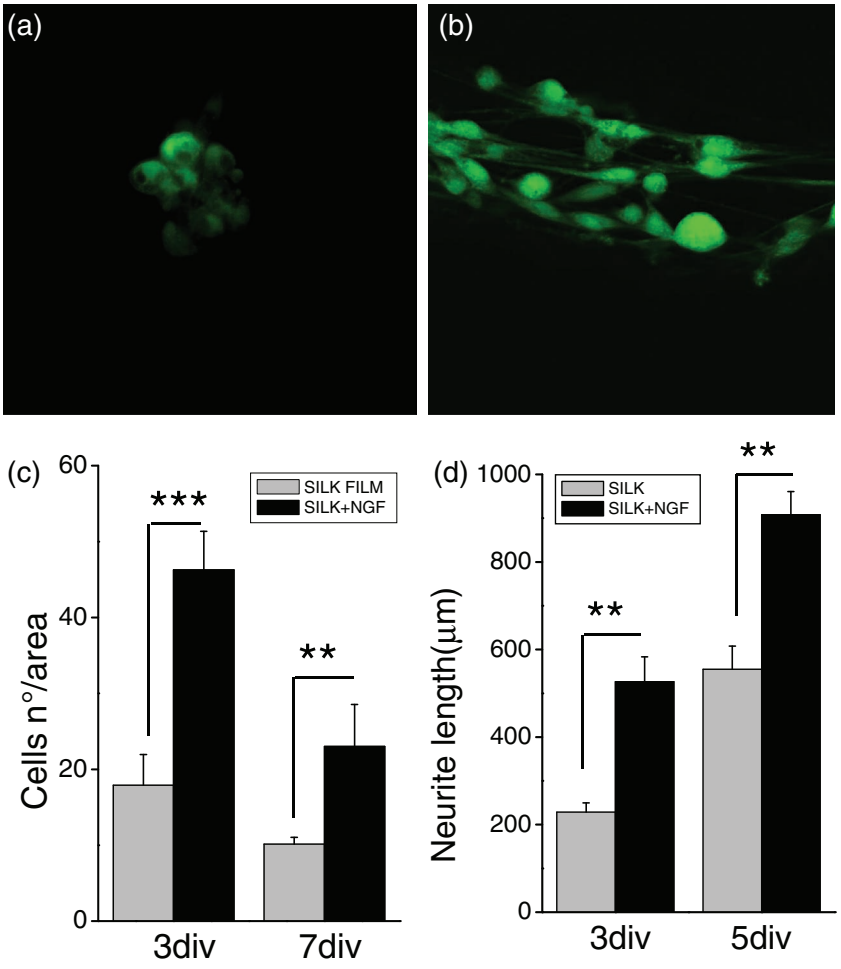

Figure 8. a,b) Single plane 20× confocal image of FDA staining of DRG cells plated on silk film (a) and on silk film+NGF (b), captured after 3 days in vitro (div). c) Histogram plot of the number of FDA positive cells/area counted in silk films (gray bars) and silk films+NGF (black bars) cell culture preparations. d) Histogram plot of neurite length measurements after 3 div and 7 div on bare silk films (gray bars) and silk films+NGF cultured neurons (black bars). Significant difference was observed in the mean values after 3 div as well as for 5 days.

Finally, we investigated the effect of silk+NGF films on DRG neuronal cell function. To this end, we performed patch-clamp and calcium imaging analyses on neurons plated on silk films and silk films+NGF, following protocols described above (see Figure 3 and Figure 7). Furthermore, we measured the typical current-clamp traces relative to voltage amplitude behavior of the first action potential evoked in SF+NGF cultured neurons in response to a pulse family of 100 ms duration (Figure 9a, left panel), or upon long lasting pulse stimulation (1 s) (Figure 9a, middle and right panels). At threshold, current values occur in silk films+NGF plated cells for single as well as repetitive firing.

A comparative analysis of the average of bioelectrical properties of different silk films (n = 8) or silk films+NGF plated neurons (n = 6) that were patched is reported in **Table 2**. The analyzed passive membrane properties were cell capacitance and V_{mem}, among others. Mean values of cell capacitance revealed that these values were lower in the silk+NGF-plated neurons compared to bare silk. Moreover, at resting value, cells were more hyperpolarized when compared to SF films. However, threshold current was significantly lower in silk+NGF-plated cells. The data on cell capacitance is in line with a more developed neurite outgrowth of silk NGF cells compared to the one observed on bare silk films (see Figure 9). The lower requirement of current (I_{th} value) for triggering the first action potential suggests a higher capability of silk+NGF plated neurons to fire.

We also analyzed $[Ca^{2+}]_i$ dynamics in silk+NGF plated cells and compared them to silk films cultured cells. Trace representative of typical $[Ca^{2+}]_i$ dynamics are reported in Figure 9b,c. Features of oscillations in dynamics and a decrease in induced desensitization were observed. Quantitative analyses of the mean values of $[Ca^{2+}]_i$ recorded before and after capsaicin in responsive cells revealed that capsaicin promoted a significant increase in $[Ca^{2+}]_I$ in DRG neurons plated on silk film+NGF with values comparable to those recorded in neurons plated on silk films. The percentage of capsaicin-responding cells was increased in the silk+NGF sample (Figure 9d). These results suggest that NGF is released by silk films[19] and that it is capable of promoting a chemosensitive reponse in DRG neurons.[59]

Collectively, the functional analyses indicate that DRG neurite outgrowth on silk films+NGF was paralleled by modulation of neuronal cell function and TRPV1-mediated chemosensitivity of sensory neurons.

3. Conclusion

SF has previously been demonstrated to be a biocompatible material for central and peripheral neural tissue growth[21,45] that can support the development of nerve conduits and is suitable for in vivo implantation.[9,20] Moreover, data regarding non-toxicity of subcutenously implanted silk-based inorganic electronic devices have been reported.[22] However, these studies did not address the effect of silk-films on the cell function, which is essential to define and control the cell–substrate interaction.

Here we have demonstrated that bare SF films support the growth and neurite extension of DRG primary sensory neurons even after several days in vitro. Moreover, we show for the first time that DRG neurons cultured on bare silk films are capable of firing and retain electrophysiological properties critical for their function in vivo. Despite a slight difference in AP amplitude, all excitability parameters measured for DRG neurons grown on silk were comparable with those recorded for neurons grown on PDL+laminin. In addition, a chemosensitive response to capsaicin, related to DRG neuron pain sensation in vivo, was

© 2012 WILEY-VCH Verlag GmbH & Co. KGaA, Weinheim

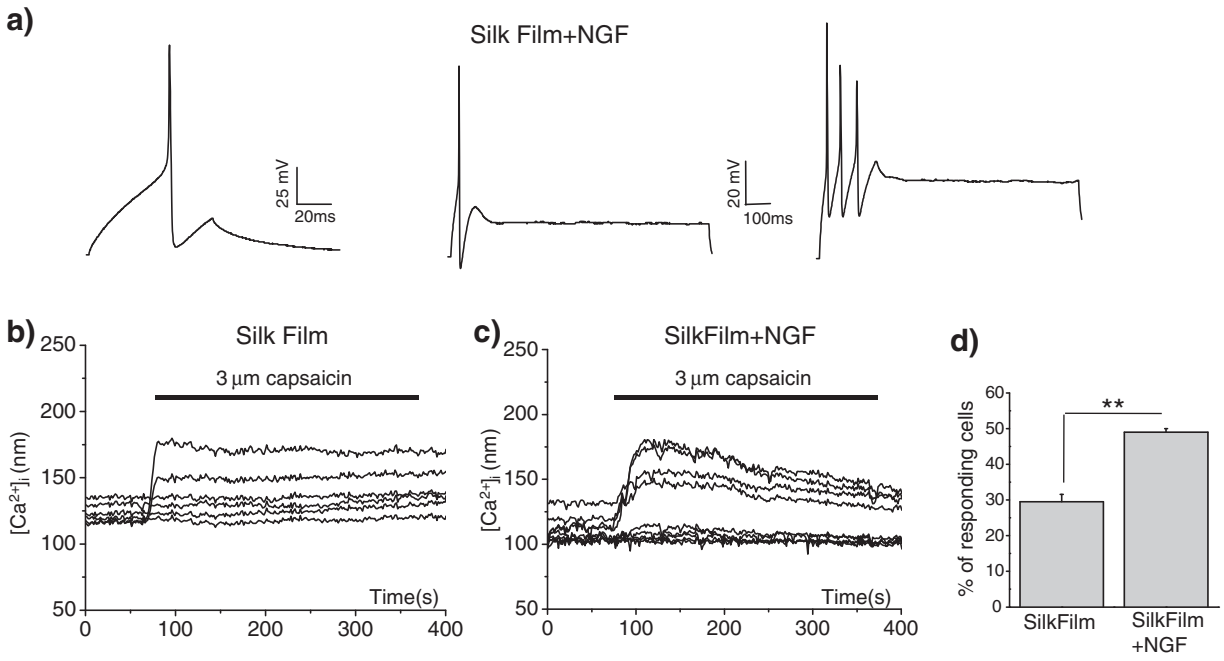

Figure 9. a) Traces representative of voltage amplitude behavior recorded in current-clamp mode of patch-clamp. The first action potential evoked from neurons cultured on silk+NGF (left panel) obtained in response to a pulse family of 100 ms duration. Central and right panels: current clamp traces obtained by long lasting pulse stimulation (1 s). Firing pattern of patched neuron was phasic firing (central) as well as repetitive firing (right) neurons. b–d) Representative traces depicting typical temporal dynamics of free intracellular Ca^{2+} concentration ($[Ca^{2+}]_i$) measured in fura-2-loaded DRG cells plated on silk films (b) or on silk films+NGF (c). Each trace corresponds to one cell analyzed in the reported representative experiment. d) Percentage of responding cells to capsaicin in silk films and silk films+NGF; mean values are relative to the percentage of responding cells in three different samples.

Table 2. Electrophysiological properties of neurons plated on silk films and silk films+NGF. Significant difference was observed in C_p values (* = $p < 0.05$), in V_{mem} (* = $p < 0.05$), and I_{th} (* = $p < 0.05$).

	C_p [pF]	Resting V_{mem} [mV]	I_{th} [nA]	V_{th} [mV]	Peak amplitude [mV]	Time to peak [ms]	AP amplitude [mV]	AHP amplitude [mV]	Max AP number pers
Silk films	27.7 ± 2.2	−65 ± 5	162 ± 20	−37 ± 2	30 ± 4	4.5 ± 1.1	67 ± 3	25 ± 2	1.2 ± 0.2
Silk films +NGF	21 ± 0.5 *	−93 ± 9 *	108 ± 11 *	−35 ± 1	36 ± 4	2.98 ± 0.4	71 ± 4	20 ± 3	2.2 ± 0.3

also observed with values in agreement with those previously reported.[33] Our findings demonstrate that SF does not negatively impact neuronal functionality and is a suitable scaffold to build an active platform in PNI therapeutic strategies.

Moreover, we demonstrated that it is possible to use silk substrates for the investigation of substances targeted to promote functional recovery of injured neurons and/or to alleviate painful disabilities, exploiting the capsaicin-mediated response. The present work further demonstrates that silk films are a suitable substrate for DRG neuron cultures as well as for studying, at the molecular level, dynamics, modulation, and functional properties of neuronal cells in response to selected molecules. In light of the recently reported integration of silk films in bioelectronic and micropatterned devices,[18,22,23,60,61] the demonstration that silk preserves biological function of neuronal cells will pave the way to the engineering of silk-based devices for functional neurite outgrowth in vitro and/or functional electrostimulation in vivo.

4. Experimental Section

Preparation of Rat Dorsal Root Ganglion Neuron Cultures: The experiments were performed according to the Italian law on the protection of laboratory animals, with the approval of a local bioethical committee and under the supervision of a veterinary commission for animal care and comfort of the University of Bologna. Every effort was made to minimize the number of animals used and their suffering.

Primary cultures of DRG neurons were prepared from post-natal p14-p18 rats according to previously described protocols.[26,27] Rat pups (Sprague Dawley) where anesthetized by alotan prior to decapitation. Approximately thirty ganglia were removed from each rat, roots were cut using microdissecting scissors, before the ganglia were transferred to ice cold phosphate buffered saline (PBS). After rinsing in Dulbecco's modified Eagle's medium (DMEM, Gibco), the ganglia were placed in DMEM containing type IV collagenase (5000 U mL^{-1}, Wentinghton) for 60–75 min at 37 °C, 5% CO_2, and then dissociated gently with some passages through 0.5 mm and 0.6 mm sterile needles. Cells were washed twice by re-suspension and centrifugation and then appropriately diluted in DMEM medium (1 mL) containing fetal bovine serum (10%, FBS, Gibco). An equal amount of cell suspension was dropped onto 12–19 mm

© 2012 WILEY-VCH Verlag GmbH & Co. KGaA, Weinheim

round, glass coverslips precoated with poly-D-lysine (50 mg mL^{-1}), followed by laminin (10 mg mL^{-1}, Sigma), or with precasted (see below) silk films and placed in a 37 °C, 5% CO_2 incubator. Cells were maintained in DMEM, Gibco added with FBS (10%) in the presence of NGF (50 ng mL^{-1}), and cytosine β-D-arabinofuranoside, (AraC, 1.5 μg mL^{-1}, Sigma) to reduce glial cell expression. Cell cultures were characterized after 72 h, 5 days, 9 days and 15 days in vitro (div), by optical imaging with a Nikon TE 2000 inverted confocal microscope equipped with a 20× objective and Hamamatsu charge-coupled device (CCD) camera. Images reported are representative of eight different cell culture preparations.

Preparation of Silk Solution and Films: Silk solutions were prepared from *Bombyx mori* silkworm cocoons (supplied by Tajima Shoji, Co.,Yokohama, Japan) according to the procedures described in previous studies.[62] The cocoons were degummed in boiling 0.02 M Na_2CO_3 (Sigma) solution for 30 min. The fibroin extract was then rinsed three times in Milli-Q water, dissolved in a 9.3 M LiBr solution yielding a 20% (w/v) silk protein solution, and subsequently dialyzed (dialysis membranes, molecular weight cutoff (MWCO) = 3500) against distilled water for 2 days to obtain a pure silk aqueous solution (ca. 8 wt/vol%). 8% silk solution was filtered twice through 0.2 μm Millipore filters (Sarsted) to generate a sterile solution. For film preparation, an aliquot (160 μL) of 8% silk solution was cast on 19 mm diameter glass coverslips, to generate films with a thickness of around 20 μm.[24,62] The as-cast silk films were desiccated for 4 h in a sterile hood. The silk-coated glass coverlips were placed in a 35 mm Petri dishes and covered with a drop of DMEM–glutamax medium with FBS (10%) and penicillin–streptomycin (100 U mL^{-1} and 100 mg mL^{-1}, respectively), and left in the incubator overnight. The next day, DRG cell culture preparations were plated in Petri dishes as described above. To prepare silk+NGF films, a NGF (50 ng mL^{-1}) containing silk fibroin solution was prepared. Silk+NGF films were prepared following the same procedure used for pure silk films.

The medium was changed every second day under all experimental conditions. Cells plated on SF+NGF were grown in media containing serum, antibiotics, and Ara-C at the same concentration as described above, avoiding addition of NGF.

Fourier Transform Infrared Spectroscopy (FT-R): The mid infrared (400–4000 cm^{-1}) absorption measurements were carried out using a Bruker IFS-88 FTIR interferometer at 4 cm^{-1} resolution averaging over 512 scans in order to improve the signal to noise ratio. Absorption spectra have been performed on SFfilms casted on infrared transparent substrates (KBr single crystals). The curve fitting of overlapping bands of the infrared spectra covering the amide I and II regions (1500–1700 cm^{-1}) were performed by using the Levenberg–Marquardt algorithm implemented in the OPUS 2.0 software for IFS-88 hardware control and spectral processing.

Silk Films Degradation Assay: SF films casted as described above were covered by cell culture media (DMEM–glutamax medium with 10% FBS and penicillin–streptomycin) then incubated in a water jacketed incubator (37 °C, 5% CO_2, relative humidity (RH) 95%) for 24 h, 3 days, 7 days, or 10 days. At appointed time points, groups of samples were rinsed in distilled water and dessicated for 1 h at 60 °C and weight at mass balance and imaged by AFM. The percentage of weight loss was considered as a representative index of SF protein degradation.[29]

Atomic Force Microscopy (AFM): The morphology of degraded SF in cell culture media solution was observed by AFM in air after drying in an oven at 60 °C for 1 h. AFM topographical images were collected using an NT-MDT Solver Scanning Probe Microscope in tapping mode with the samples kept in air.

Neurite Length: The neurite mean length was determined by measuring the length of neurite quantified under bright field image at 400× by means of a commercial software (ImageJ). Ten fields containing at least three identifiable DRG neurons were captured for each sample. Data are representative of three independent experiments carried out in duplicate.

Immunofluorescence: DRG cultures plated on different coverslips were fixed with paraformaldehyde (4%) in PBS (0.1 M) for 10–15 min at room temperature (RT, 20–24 °C). After blocking with bovine serum albumin (BSA, 3%) in PBS for 15 min at RT, cells were incubated overnight with mouse anti-NeuN (Millipore) or mouse-anti-GAP43 (Sigma-Aldrich) affinity-purified antibodies (diluted 1:100) in blocking solution to which Triton X100 (0.1%) was added. The day after, cells were incubated with Alexa Fluor 488-conjugated donkey anti-mouse or Alexa Fluor 595-conjugated donkey anti-mouse antibodies (Molecular Probes-Invitrogen, diluted 1:1000) in blocking solution containing Triton X100 (0.1%). Coverslips were then mounted with Prolong Anti-Fade (Molecular Probes-Invitrogen) and optically imaged with a Nikon TE 2000 inverted confocal microscope equipped with a 40× or 60× oil-objective and 400 nm diode, 488 nm Ar^+, and 543 nm He–Ne lasers as excitation sources.

Ten to twelve micrometric images were captured of NeuN positive cells with a 20× objective. The average number of NeuN positive cells per area (0.3 mm × 0.3 mm) was calculated. Data reported has been obtained by two different experiments in duplicate.

Electrophysiology: Current recordings were obtained with the whole-cell configuration of the patch-clamp technique. Patch pipettes were prepared from thin-walled borosilicate glass capillaries to have a tip resistance of 2-4 MΩ when filled with the standard internal solution. Membrane currents were amplified (List EPC-7) and stored on a computer for off-line analysis (pClamp 6, Axon Instrument and Origin 6.0, MicroCal). Because of the large current amplitude, access resistance (below 10 MΩ) was corrected 70–90%. Experiments were performed after 3–4 div. The rationale of choosing this time interval was due to the fact that DRG neuron are known to change their electrophysiological properties within several days in culture, depending on cell culture treatment.[63] Experiments were carried out at RT (20–24 °C). Because DRG primary neurons are a heterogeneous cell population,[48,54] neurons with a small diameter (<30 μm) were selected to perform a comparative analyses between two experimental conditions.[54] Action potential (AP) and neuronal firing were recorded in current clamp mode by injecting repetitive increasing current pulse from –0.05 to 0.350 nA of 100 ms duration. Capacitative transients were cancelled by compensation by nulling the circuit of the recording amplifier. V_{mem} was measured 1 min after a stable recording was obtained. I_{th} was defined as the minimum current required to evoke an AP. The AP V_{th} was defined as the first point on the upstroke of an AP. The AP amplitude was measured between the peak and AP threshold level. The AP rising time to peak was defined as the time for rising from baseline to the AP peak. The AHP amplitude was measured between the maximum hyperpolarization and the final plateau voltage. All cells without AP were excluded from the study.

The maximal number of firing was calculated by counting the number of overshooting AP in response to a 1 s pulse of current injection.[53] Whole-cell *I–V* curves for individual neurons were generated by calculating the mean of the maximal inward and outward current values recorded at each potential and normalized for the relative cell capacitance values.

Intracellular Calcium Microfluorometry: Variations in intracellular free Ca^{2+} concentration ($[Ca^{2+}]_i$) were monitored by ratiometric microfluorometry using fluorescent Ca^{2+} indicator fura-2 AM. Before measurements, DRG cell culture preparations seeded in silk film-coated coverslips were loaded with fura-2 AM (10 μM), dissolved in standard bath solution (see below), for 45 min at 25 °C. For microfluorometric analysis cell coverslips were mounted in a perfusion chamber containing bath saline (100 μL). Cells were continuously perfused at a rate of 1 mL min^{-1} with different saline. Measurements of $[Ca^{2+}]_i$ in single cells were performed with an inverted fluorescence microscope Nikon Eclipse TE2000U equipped with long-distance dry objective (40×) and appropriate filters. The emission fluorescence of selected cell was passed through a 510 nm narrow-band filter and acquired with a digital charge-coupled device camera (VTi, VisiTech International Ltd., Sunderland, UK). Monochromator settings, chopper frequency, and complete data acquisition were controlled by QuantiCell 2000 (VisiTech). The excitation wavelength was alternated between 340 and 380 nm with a sampling rate of 0.25 or 0.5 Hz. Fluorescence ratio measured at 340 nm and 380 nm (F340/F380) was used as an indicator of $[Ca^{2+}]_i$ changes. The calibration of the F340/F380 nm ratio in terms of free Ca^{2+} concentration was based

© 2012 WILEY-VCH Verlag GmbH & Co. KGaA, Weinheim

on the procedure described previously.[64] Quantitative conversion of ratiometric measurement to $[Ca^{2+}]_i$ was performed off-line by QuantiCell 2000.

To calculate capsaicin response, changes in $[Ca^{2+}]_i$ greater than the 10% of the control value were considered as referred to capsaicin responding cells and the value was taken into account for mean calculation. The number of responding cells was normalized to the total number of imaged cells in the area analyzed.

Solutions and Chemicals: All salts and chemicals employed for the investigations were of the highest purity grade (Sigma). For electrophysiological and calcium imaging experiments the standard bath saline was: NaCl (140 mM), KCl (4 mM), $MgCl_2$ (2 mM), $CaCl_2$ (2 mM), 4-(2-Hydroxyethyl)piperazine-1-ethanesulfonic acid (10 mM), *N*-(2-hydroxyethyl)piperazine-*N*′-(2-ethanesulfonic acid) (HEPES, 10 mM), glucose (5 mM), pH 7.4 with NaOH and osmolarity adjusted to ≈315 mOsm with mannitol. The intracellular (pipette) solution was composed of: KCl (144 mM), $MgCl_2$ (2 mM) NaATP (2 mM), ethylene glycol-bis(2-aminoethylether)-*N,N,N′,N′*-tetraacetic acid (EGTA, 5 mM), 4-(2-hydroxyethyl)-1-piperazineethanesulfonic acid (HEPES,10 mM), pH 7.2 with KOH and osmolarity ≈300 mOsm. For electrophysiological experiments extracellular saline was applied with a gravity-driven, local perfusion system at a flow rate of ≈200 µL min^{-1} positioned within ≈100 µm of the recorded cell. Capsaicin was dissolved in dimethyl sulfoxide (DMSO) at a concentration 10 000 times higher than the one used and kept at –20 °C.

Statistical Methods: Results were statistically analyzed using one-way analysis of variance (ANOVA) or Independent *t*-student test. A statistically significant difference was reported if $p < 0.05$. Data were reported as the mean ± standard error (SE) from at least three separate experiments.

Acknowledgements

V.B. and K.S. conbributed equally to this work. This work was supported by EU project FP7-ICT- 248052 (PHOTO-FET), by Consorzio MIST E-R through Programma Operativo FESR 2007-2013 della Regione Emilia-Romagna–Attività I.1.1, and by Italian MIUR project FIRB-RBPR05JH2 (ITALNANONET). The authors also thank the NIH P41 Tissue Engineering Resource Center (P41 EB002520) for partial financial support. The authors gratefully acknowledge the skillfull technical support of Marco Caprini and Alessia Minardi, Dept. of Human and General Physiology, University of Bologna, for DRG cell culture preparation and maintenance.

Received: September 27, 2011
Published online: February 20, 2012

[1] P. Fromherz, in *Nanoelectronics and Information Technology*, (Ed: R. Waser), Wiley-VCH Verlag, Berlin **2003**, 781.
[2] A. Poghossian, S. Ingebrandt, A. Offenhäusser, M. J. Schöning, *Semin. Cell Dev. Biol.* **2009**, *20*, 41.
[3] W. Wang, J. L. Collinger, M. A. Perez, E. C. Tyler-Kabara, L. G. Cohen, N. Birbaumer, S. W. Brose, A. B. Schwartz, M. L. Boninger, D. J. Weber, *Phys. Med. Rehabil. Clin. N. Am.* **2010**, *21*, 157.
[4] G. Voskerician, M. S. Shive, R. S. Shawgo, H. von Recum, J. M. Anderson, M. J. Cima, R. Langer, *Biomaterials* **2003**, *24*, 1959.
[5] C. J. Bettinger, Z. Bao, *Adv. Mater.* **2010**, *22*, 651.
[6] C. E. Schmidt, V. R. Shastri, J. P. Vacanti, R. Langer, *Proc. Natl. Acad. Sci. USA* **1997**, *94*, 8948.
[7] M. Irimia-Vladu, P. A. Troshin, M. Reisinger, L. Shmygleva, Y. Kanbur, G. Schwabegger, M. Bodea, R. Schwödiauer, A. R. Mumyatov, J. W. Fergus, V. F. Razumov, H. Sitter, N. Serdar Sariciftci, S. Bauer, *Adv. Funct. Mater.* **2010**, *20*, 4069.
[8] O. Alluin, C. Wittmann, T. Marqueste, J. F. Chabas, S. Garcia, M. N. Lavaut, D. Guinard, F. Feron, P. Decherchi, *Biomaterials* **2009**, *30*, 363.
[9] Y. Yang, F. Ding, J. Wu, W. Hu, W. Liu, J. Liu, X. Gu, *Biomaterials* **2007**, *28*, 5526.
[10] N. Sinis, A. Kraus, N. Tselis, M. Haerle, F. Werdin, H. E. Schaller, *J Brachial. Plex. Peripher. Nerve Inj.* **2009**, *4*, 19.
[11] S. G. Zencirci, M. D. Bilgin, H. Yaraneri, *J. Neurosci. Methods* **2010**, *191*, 277.
[12] I. Klusáková, P. Dubový, *Ann. Anat.* **2009**, *191*, 248.
[13] G. Melli, A. Höke, *Expert. Opin. Drug Discovery* **2009**, *4*, 1035.
[14] R. Baron, *Handbook Exp. Pharmacol.* **2009**, *194*, 3.
[15] H. Ueda, *Pharmacol. Ther.* **2006**, *109*, 57.
[16] G. H. Altman, F. Diaz, C. Jakuba, T. Calabro, R. L. Horan, J. Chen, H. Lu, J. Richmond, D. L. Kaplan, *Biomaterials* **2003**, *24*, 401.
[17] C. Vepari, D. L. Kaplan, *Prog. Polym. Sci.* **2007**, *32*, 991.
[18] R. Capelli, J. J. Amsden, G. Generali, S. Toffanin, V. Benfenati, M. Muccini, D. L. Kaplan, F. G. Omenetto, R. Zamboni, *Org. Electron.* **2011**, *12*, 1146.
[19] L. Uebersax, M. Mattotti, M. Papaloïzos, H. P. Merkle, B. Gander, L. Meinel, *Biomaterials* **2007**, *28*, 4449.
[20] S. Madduri, M. Papaloïzos, B. Gander, *Biomaterials* **2010**, *31*, 2323.
[21] Y. Yang, X. Chen, F. Ding, P. Zhang, J. Liu, X. Gu, *Biomaterials* **2007**, *28*, 1643.
[22] D. H. Kim, J. Viventi, J. J. Amsden, J. Xiao, L. Vigeland, Y. S. Kim, J. A. Blanco, B. Panilaitis, E. S. Frechette, D. Contreras, D. L. Kaplan, F. G. Omenetto, Y. Huang, K. C. Hwang, M. R. Zakin, B. Litt, J. A. Rogers, *Nat. Mater.* **2010**, *9*, 511.
[23] D. H. Kim, Y. S. Kim, J. Amsden, B. Panilaitis, D. L. Kaplan, F. G. Omenetto, M. R. Zakin, J. A. Rogers, *Appl. Phys. Lett.* **2009**, *95*, 133701.
[24] V. Benfenati, S. Toffanin, R. Capelli, L. M. Camassa, S. Ferroni, D. L. Kaplan, F. G. Omenetto, M. Muccini, R. Zamboni, *Biomaterials* **2010**, *31*, 7883.
[25] C. Aurilio, V. Pota, M. C. Pace, M. B. Passavanti, M. Barbarisi, *J. Cell. Physiol.* **2008**, *215*, 8.
[26] M. F. Pazyra-Murphy, R. A. Segal, *J. Visualized Exp.* **2008**, *20*, 951.
[27] T. H Burkey, C. M. Hingtgen, M. R.Vasko, *Methods Mol. Med.* **2004**, *99*, 189.
[28] L. S. Premkumar, P. Sikand, *Curr. Neuropharmacol.* **2008**, *6*, 151.
[29] Q. Lu, B. Zhang, M. Li, B. Zuo, D. L. Kaplan, Y. Huang, H. Zhu, *Biomacromolecules* **2011**, *12*, 1080.
[30] R. L. Horan, K. Antle, A. L. Collette, Y. Wang, J. Huang, J. E. Moreau, V. Volloch, D. L. Kaplan, G. H. Altman, *Biomaterials* **2005**, *26*, 3385.
[31] E. Kharlampieva, V. Kozlovskaya, B. Wallet, V. V. Shevchenko, R. R. Naik, R. Vaia, D. L. Kaplan, V. V. Tsukruk, *ACS Nano* **2010**, *4*, 7053.
[32] F. Greve, S. Freker, A. G. Bittermann, C. Burkhardt, A. Hierlemann, H. Hall, *Biomaterials* **2007**, *28*, 5246.
[33] P. Cesare, P. McNaughton, *Proc. Natl. Acad. Sci. USA* **1996**, *93*, 15435.
[34] B. D. Birch, D. L. Eng, J. D. Kocsis, *Proc. Natl. Acad. Sci. USA* **1992**, *89*, 7878.
[35] K. L. Lankford, S. G. Waxman, J. D. Kocsis, *J. Comp. Neurol.* **1998**, *391*, 11.
[36] S. Di Giovanni, A. De Biase, A. Yakovlev, T. Finn, J. Beers, E. P. Hoffman, A. I. Faden, *J. Biol. Chem.* **2005**, *280*, 2084.
[37] R. P. Singh, Y. H. Cheng, P. Nelson, F. C. Zhou, *Cell Transplant* **2009**, *18*, 55.
[38] C. E. Van der Zee, H. B. Nielander, J. P. Vos, S. Lopes da Silva, J. Verhaagen, A. B. Oestreicher, L. H. Schrama, P. Schotman, W. H. Gispen, *J. Neurosci.* **1989**, *9*, 3505.
[39] R. V. Bellamkonda, *Biomaterials* **2006**, *27*, 3515.
[40] J. S. Belkas, M. S. Shoichet, R. Midha, *Neurol. Res.* **2004**, *26*, 151.

© 2012 WILEY-VCH Verlag GmbH & Co. KGaA, Weinheim

[41] V. B. Doolabh, M. C. Hertl, S. E. Mackinnon, *Rev. Neurosci.* **1996**, *7*, 47.
[42] L. A. Pfister, M. Papaloizos, H. P. Merkle, B. Gander, *J. Peripher. Nerv. Syst.* **2007**, *12*, 65.
[43] S. Cunha, S. Panseri, S. Antonini, *Nanomedicine* **2011**, *7*, 50.
[44] A. Volterra, J. Meldolesi, *Nat. Rev. Neurosci.* **2005**, *6*, 626.
[45] X. Tang, F. Ding, Y. Yang, N. Hu, H. Wu, X. Gu, *J. Biomed. Mater. Res. A.* **2009**, *91*, 166.
[46] L. D. Acevedo, Z. Galdzicki, A. R. McIntosh, S.I. Rapoport, *Brain Res.* **1995**, *701*, 89.
[47] A. Sculptoreanu, W. C. de Groat, *Exp. Neurol.* **2007**, *205*, 92.
[48] P. K. Tripathi, L. Trujillo, C. A. Cardenas, C. G. Cardenas, A. J. de Armendi, R. S. Scroggs, *Neuroscience* **2006**, *143*, 923.
[49] M. A. Johnson, J. P. Weick, R. A Pearce, S. C. Zhang, *J. Neurosci.* **2007**, *27*, 3069.
[50] T. R. Cummins, J. A. Black, S. D. Dib-Hajj, S. G. Waxman, *J. Neurosci.* **2000**, *20*, 8754.
[51] X. F. Zhang, M. Gopalakrishnan, C. C. Shieh, *Neuroscience* **2003**, *122*, 1003.
[52] X. F Zhang, C. Z. Zhu, R. Thimmapaya, W. S. Choi, P. Honore, V. E. Scott, P. E. Kroeger, J. P. Sullivan, C. R. Faltynek, M. Gopalakrishnan, C.-C. Shieh, *Brain. Res.* **2004**, *1009*, 147.
[53] T. R. Cummins, A. M. Rush, M. Estacion, S. D. Dib-Hajj, S. G. Waxman, *Nat. Protocols* **2009**, *4*, 1103.
[54] C. L. Stucky, G. R. Lewin, *J. Neurosci.* **1999**, *19*, 6497.
[55] L. J. Hudson, S. Bevan, G. Wotherspoon, C. Gentry, A. Fox, J. Winter, *Eur. J. Neurosci.* **2001**, *13*, 2105.
[56] V. Vellani, S. Mapplebeck, A. Moriondo, J. B. Davis, P. A. McNaughton, *J. Physiol.* **2001**, *534*, 813.
[57] E. Palazzo, L. Luongo, V. de Novellis, L. Berrino, F. Rossi, S. Maione, *Mol. Pain* **2010**, *6*, 66.
[58] M. J. Caterina, A. Leffler, A. B. Malmberg, W. J. Martin, J. Trafton, K. R. Petersen-Zeitz, M. Koltzenburg, A. I. Basbaum, D. Julius, *Science* **2000**, *288*, 306.
[59] S. Bevan, J. Winter, *J. Neurosci.* **1995**, *15*, 4918.
[60] H. Perry, A. Gopinath, D. L. Kaplan, L. Dal Negro, F. G. Omenetto, *Adv. Mater.* **2008**, *20*, 3070.
[61] C. H. Wang, C. Y. Hsieh, J. C. Hwang, *Adv. Mater.* **2011**, *23*, 1630.
[62] B. D. Lawrence, F. Omenetto, K. Chui, D. L. Kaplan, *J. Mater. Sci.* **2008**, *43*, 6967.
[63] L. G. Aguayo, G. White, *Brain Res.* **1992**, *570*, 61.
[64] G. Grynkiewicz, M. Poenie, R. Y. Tsien, *J. Biol. Chem.* **1985**, *260*, 3440.

© 2012 WILEY-VCH Verlag GmbH & Co. KGaA, Weinheim